3D modeling of material heating with the laser beam for cylindrical geometry

Radovan Gospavic [a,*], Milesa Sreckovic [b], Viktor Popov [c], Goran Todorovic [a]

[a] *Faculty of Civil Engineering, Bulevar Kralja Aleksandra 73, Belgrade, Serbia and Montenegro*
[b] *Faculty of Electrical Engineering, Bulevar Kralja Aleksandra 73, Belgrade, Serbia and Montenegro*
[c] *Wessex Institute of Technology, Ashurst Lodge, Ashurst, Southampton SO40 7AA, UK*

Abstract

In this work an analytical approach for analyzing heating of material with a laser beam is presented. A thermal model of interaction for the case of cylindrical geometry of the material and asymmetric distribution of the laser beam intensity is used and an analytical procedure is developed to analyze the temporal and the spatial distribution of the temperature field inside the bulk of material. This kind of consideration is of practical interest in cases where the excitation by the laser beam is not symmetric in respect to its position or shape, e.g., multi-mode working regimes or asymmetrical distribution of the laser beam intensity. The heating effects were considered in the temperature range up to the melting point. The thermal and the optical parameters of the material were assumed to be independent of the temperature and were given constant values in the temperature range of interest.

This approach makes use of the Laplace transform, in order to eliminate dependence on time. The Fourier method of variable separation was used to obtain the temperature field distribution in the Laplace transform domain. By using the pulse response and Duhamel's principle the 3D temperature field distribution in time domain is obtained. By using an appropriate set of orthogonal functions in r directions, the numerical procedure is made more effective, saving this way the CPU time.

The general solutions for the temporal as well as spatial temperature field distributions are evaluated in a closed form in terms of the particular solutions of the governing partial differential equation (PDE). Because of linearity of the governing PDE, the superposition principle was used in the case of complex distributions of the laser beam intensity. The influence of different kinds of laser beam parameters to the temperature field distributions was considered.

1. Introduction

In a general case the analysis of the laser–material interaction, important for practical applications, is very complex and includes analysis of different physical processes such as material removal, material melting, thermal stresses, shock wave, etc. This prevents successful construction of a general analytical solution and different numerical procedures have been used in the past [1]. This work is restricted only to analysis of heating effects of the

* Corresponding author. Tel.: +381 11 324 8464; fax: +381 11 324 8681.
  E-mail address: gospavic@grf.bg.ac.yu (R. Gospavic).

laser–material interaction. In many practical applications of laser beams the finite dimensions of the bulk material and the asymmetric distribution of the laser beam intensity has to be taken into account. The presented analytical approach enables consideration of the heating effects of interactions for the different and complicated laser-beam distributions for cases without axial symmetry. The temperature field distribution in this way can be analyzed for 3D cylindrical geometry allowing monitoring of the time evolution of the temperature distribution. For the arbitrary time dependence, spatial distribution and position of the incoming laser beam intensity the same numerical data could be used, saving in this way memory and CPU time. By using Duhamel's principle [2] the temperature distribution is evaluated by using the convolution integral.

This kind of analyses could be important in many technical applications of laser beams in technology and science [3–5] as well as in the case of laser–material interaction in the multi-mode working regime.

In general the consideration of the thermal effects of interaction could be of interest from the aspect of the analyses of heating of different optical components by the laser beam, too.

For the multi-mode working regime as well as for the complex laser beam intensity distribution the superposition principle could be used. In case of the linear governing partial differential equation (PDE) the final solution could be presented as a superposition or sum of the PDE solutions belonging to different parts of the incident loads, i.e. in our case the incoming laser beam intensity.

Also, this approach could be of interest in cases when the focus of the incoming laser beam is not aligned with the axis of the cylindrical object.

The advantage of the semi-analytical approach relative to a numerical one, is that the 3D space and temporal temperature distribution for a specific geometry is evaluated in a closed form without need for a meshing process [6,7].

Also, the temperature could be obtained in an arbitrary single point at any time inside the bulk of the material while in a numerical approach the temperature distribution is usually evaluated in a predefined set of points within the problem domain.

2. Mathematical model

Heating of a homogeneous cylinder, with a finite or infinite length, by an incident laser beam on the upper surface of the specimen is considered (Fig. 1). The shape of the cross-section, the position of the laser beam on the upper side of the specimen, the distribution and the time dependence of the laser beam intensity can be arbitrary. In the numerical examples presented in this paper, because of simplicity and still without losing generality, only a top head laser beam profile with circular cross section is considered. It was assumed that the laser beam intensity could be approximated by a product of two functions of spatial and time coordinates: $q(r)$ and $\varphi(t)$, respectively [5,8].

Only the heating effects due to the interaction were considered. The laser–material interaction was modeled by the equivalent thermal flux on the upper side of the specimen. All thermal and optical parameters of the material are considered to be constant and temperature independent, yielding a linear thermal conduction problem. The geometry of the considered problem was represented in a cylindrical reference system.

Only temperature distribution inside the bulk material is considered. The convective thermal losses from the lower and the axial surfaces of the material were taken into account, while the thermal losses from the upper surface of the specimen are neglected. The radiative losses have important contributions to the whole thermal losses at the very high temperatures [8].

Thus, for low temperature of the specimen, the radiative heat losses are smaller than convective ones and could be neglected [8]. Beside this, if the absorption length, for the considered laser beam and material, is very short, relative to the size of the heating affected zone (HAZ), it could be considered that the laser beam is absorbed by the surface of the specimen. This is the case for many materials of interest, thus the laser–material interaction could be approximated by the equivalent surface thermal source [8]. Also, a constant and temperature independent value of the coefficient of thermal conductivity was assumed.

Once these approximations are applied, the heating of the considered cylindrical specimen can be modeled by the following PDE and the corresponding boundary (BC) and initial (IC) conditions [5,9]:

$$\frac{\partial^2 T}{\partial r^2} + \frac{1}{r}\frac{\partial T}{\partial r} + \frac{\partial^2 T}{\partial z^2} + \frac{1}{r^2}\frac{\partial^2 T}{\partial \theta^2} = \frac{1}{\alpha}\frac{\partial T}{\partial t}; \quad t \geq 0, \quad 0 \leq r \leq R, \quad 0 \leq z \leq H, \quad 0 \leq \theta \leq 2\pi, \tag{1a}$$

$$-\lambda \left.\frac{\partial T(r,z,\theta,t)}{\partial z}\right|_{z=0} = A \cdot q(r,\theta) \cdot \phi(t); \quad -\lambda \left.\frac{\partial T(r,z,\theta,t)}{\partial r}\right|_{r=R} = h_c \cdot T(r,z,\theta,t)|_{r=R};$$
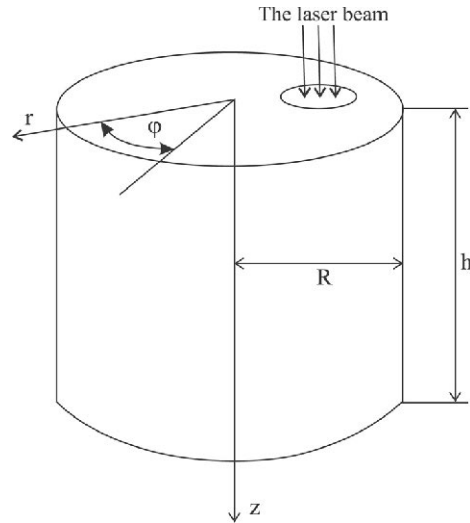
Fig. 1. The geometry of the considered problem and coordinate system used.

$$-\lambda \left.\frac{\partial T(r,z,\theta,t)}{\partial z}\right|_{z=H} = h_c \cdot T(r,z,\theta,t)|_{z=H}, \tag{1b}$$

$$T(r,z,\theta,t=0) = 0; \quad 0 \le r \le R, \quad 0 \le z \le H, \quad 0 \le \theta \le 2\pi, \tag{1c}$$

where: λ is the coefficient of thermal conductivity, which is considered to be constant and temperature independent, $\alpha = \lambda/\rho \cdot c$ is the thermal diffusivity, c is the specific heath, ρ is the material density, h_c is the heat transfer coefficient [10], A is the absorption coefficient of the laser radiation by the material [11], R, h are the radius and length of the specimen, respectively, and T is the temperature difference in the interior domain relative to the ambient one. Eq. (1b) represents the homogeneous BCs while Eq. (1c) describes the IC.

The Laplace transform approach was used to eliminate the time dependence and to convert the original problem to the equivalent problem in the Laplace transform domain [12]. Fourier's method of variable separation was used in order to transform the original PDE into three ordinary differential equations as follows [12]:

$$r^2\frac{\partial^2 T_r(r)}{\partial r^2} + r\frac{\partial T_r(r)}{\partial r} + (\mu^2 \cdot r^2 - m^2)T_r(r) = 0,$$
$$\frac{\partial^2 T_z^*(z,s)}{\partial z^2} - \left(\mu^2 + \frac{s}{\alpha}\right) \cdot T_z^*(z,s) = 0, \tag{2}$$
$$\frac{\partial^2 T_\theta(\theta)}{\partial \theta^2} + m^2 T_\theta(\theta) = 0; \quad T^*(r,z,\theta,s) = T_r(r) \cdot T_\theta(\theta) \cdot T_z^*(z,s),$$

where μ and m are constants, s is a complex parameter, and the asterisk in the superscript denotes functions in Laplace's transform domain. The particular solutions of the governing PDE can be expressed in the following form in the Laplace transform domain [9,13,14]:

$$T_{mn}^*(r,z,\theta,s) = T_r(r) \cdot T_\theta(\theta) \cdot T_{zmn}^*(z,s);$$
$$T_r(r) = J_m(\mu_{mn} \cdot r); \quad T_\theta(\theta) = K_{1m}\cos(m \cdot \theta) + K_{2m}\sin(m \cdot \theta); \quad n = 1,2,\ldots, \tag{3}$$

where m is integer, $T(\theta) = T(\theta + 2m\pi)$, because of the continuity condition, J_m are Bessel functions of the m-th kind and μ_{mn} are positive roots of the characteristic transcendent equations which describe the BC on the axial boundary surface of the specimen, given by the next relation:

$$-\lambda\frac{\mu_{mn}}{2}(J_{m+1}(\mu_{mn}R) - J_{m-1}(\mu_{mn}R)) = h_c \cdot J_m(\mu_{mn}R). \tag{4}$$
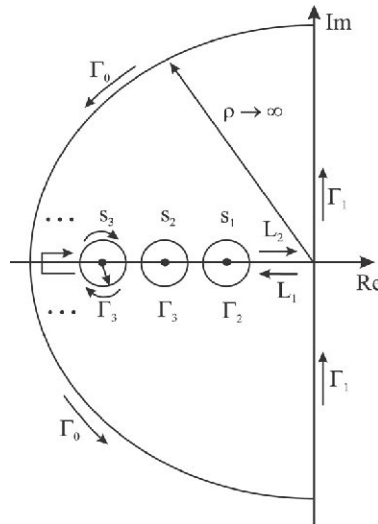
Fig. 2. The contour of integration used in evaluating the Bromwich integral in (10), where $s_1, s_2, \ldots$ are poles of the complex function $T^*(r, z, \theta, s)$ in (10) given by the relation (9).
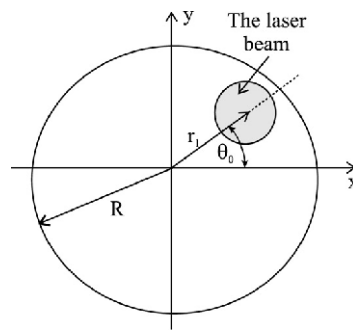
Fig. 3. Position of the laser beam on upper surface of the specimen.

Also, the next relations hold: $\mu_{m,-n} = -\mu_{mn}$, $(\mu_{mn} \geq 0)$ and $T^*_{rm-n} = (-1)^{-m} T^*_{rmn}$. Due to the boundary conditions on the lower surface of the specimen and according to previous work [9], $T^*_{zmn}(z, s)$ could be expressed in the following way:

$$T^*_{zmn}(z, s) = T^*_{0mn}(s) \cdot \left(\exp\left(\frac{iz \cdot \varepsilon}{h} \right) + \frac{i\lambda \cdot \varepsilon/h + h_c}{i\lambda \cdot \varepsilon/h - h_c} \exp\left(i\frac{2 \cdot h - z}{h}\varepsilon \right) \right); \quad i\varepsilon = h\sqrt{\mu_{mn}^2 + \frac{s}{\alpha}}. \tag{5}$$

If the laser beams have rounded cross-section and top head profile, because of symmetry the particular solutions given by (2) have to be odd functions of the angular coordinate θ (Fig. 3) and accordingly K_{1m} and K_{2m} in (2) can be $K_{1m} = 1$ and $K_{2m} = 0$.

As the particular solutions, for positive values of the constants μ_{mn}, are linearly independent, the solution in the Laplace transform domain could be evaluated by the series of the particular ones:

$$T^*(r, z, \theta, s) = \sum_{n=1}^{+\infty} \sum_{m=0}^{+\infty} a_{mn} \cdot T_{rmn}(r) \cdot T_{\theta m}(\theta) \cdot T^*_{zmn}(z, s), \tag{6a}$$

$$T^*(r, z, \theta, s) = \sum_{n=1}^{+\infty} \sum_{m=0}^{+\infty} J_m(\mu_{mn} \cdot r) \cdot (a_{1mn} \cdot \cos(m \cdot \theta) + a_{2mn} \cdot \sin(m \cdot \theta)) \cdot T^*_{zmn}(z, s),$$

$$a_{1mn} = a_{mn} \cdot K_{1m}; \quad a_{2mn} = a_{mn} \cdot K_{2m}. \tag{6b}$$

In (6a) and (6b) only the first N terms in the series need to be evaluated numerically, while the rest of the terms, for sufficiently large N, can be omitted. The products of unknown constants a_{1mn}, a_{2mn} and $T^*_{0mn}(s)$ could be determined by the BC on the upper surface of the specimen. It is assumed that the time dependence of the laser beam intensity is given by Dirac's function. The spatial distribution of the intensity $q(r, \theta)$ could be expanded for a 2D domain in Fourier's series of orthogonal functions. Also, $T_r(\mu_{mn} \cdot r)$ can be expanded on the interval $[0, R]$ in a series of orthogonal Bessel functions of m-th kind (J_m) in the following way [12]:

$$q(r, \theta) = \sum_{m=0}^{N} (q_{1m}(r) \cdot \cos(m \cdot \theta) + q_{2m}(r) \cdot \sin(m \cdot \theta)), \tag{7a}$$

$$q_{1m}(r) = \sum_{i=1}^{N} q_{1mi} \cdot J_m(p_i \cdot r); \quad q_{2m}(r) = \sum_{i=1}^{N} q_{2mi} \cdot J_m(p_i \cdot r); \quad J_m(p_{mi} \cdot R) = 0;$$

$$(r, \theta) \in D; \quad D = \{(r, \theta) \mid r \in [0, R], \theta \in [0, 2\pi]\}, \tag{7b}$$

$$J_m(\mu_{mn} \cdot r) = \sum_{i=1}^{N} b_{mni} \cdot J_m(p_i \cdot r); \quad b_{mni} = \frac{2 \cdot p_{mi} \cdot J_{m-1}(p_{mi}R) \cdot J_m(\mu_{mn}R)}{R(\mu_{mn}^2 - p_{mi}^2) \cdot J_{m+1}^2(p_{mi}R)}, \tag{7c}$$

where q_{mi} are constants in 2D Fourier's expansions of $q(r, \theta)$, b_{mni} is a tensor of third order and represents the constants in the expansions of $J_m(\mu_{mn} \cdot r)$ on interval $[0, R]$ in a series of orthogonal Bessel functions of m-th kind. In (7) only the first N terms in the expansions are taken into account. The orthogonal functions for the r direction could be arbitrary, but the best choice are orthogonal Bessel functions of m-th kind (J_m), for q_{1m} and q_{2m}, because in that case the tensor b_{mni} could be evaluated in closed form, as could be seen in Eq. (7c). In other words, for each new value of index m, a new orthogonal set of base functions (J_m) was used. In this way the numerical procedure becomes faster, this way saving CPU time, while a sufficient number of terms could be taken into account in (6b).

The unknown coefficients in (6a) and (6b) could be evaluated by using the BC on the upper surface of the specimen. The following series of linear equations were solved simultaneously and the unknown coefficients were found in the following way:

$$B_m \cdot C_{1m} = Q_{1m}; \quad B_m \cdot C_{2m} = Q_{2m}; \Rightarrow C_{1m} = B_m^{-1} \cdot Q_{1m}; \quad C_{2m} = B_m^{-1} \cdot Q_{2m};$$

$$B_m = [b_{\min}]_{N \times N}; \quad B_m^{-1} = [b_{\min}^{-1}]_{N \times N}; \quad Q_{1m} = [q_{1mi}]_{N \times 1}; \quad Q_{2m} = [q_{2mi}]_{N \times 1}; \tag{8a}$$

$$C_{1m} = [c_{1mi}]_{N \times 1}; \quad C_{2m} = [c_{2mi}]_{N \times 1},$$

$$a_{1mn} T^*_{0mn} = \frac{A \cdot c_{1mn} \cdot (i\lambda\varepsilon/h - h_c) \cdot \exp(-i\varepsilon)}{i\lambda\varepsilon/h \cdot g(\varepsilon)}; \quad a_{2mn} T^*_{0mn} = \frac{A \cdot c_{2mn} \cdot (i\lambda\varepsilon/h - h_c) \cdot \exp(-i\varepsilon)}{i\lambda\varepsilon/h \cdot g(\varepsilon)} \tag{8b}$$

$$g(\varepsilon) = (i\lambda\varepsilon/h + h_c) \cdot \exp(i\varepsilon) - (i\lambda\varepsilon/h - h_c) \cdot \exp(-i\varepsilon),$$

$$c_{1mn} = \sum_{i=1}^{N} q_{1mi} \cdot b_{\min}^{-1}; \quad c_{2mn} = \sum_{i=1}^{N} q_{2mi} \cdot b_{\min}^{-1}. \tag{8c}$$

In (8b) ε has the same meaning as in expression (5). The poles of the function $T^*(r, z, \theta, s)$ could be obtained as roots of the next characteristic transcendent equation [9]:

$$g(\varepsilon) = 0 \Rightarrow \varepsilon_j \cdot tg\varepsilon_j = \frac{h \cdot h_c}{\lambda}; \quad s_{jmn} = -\alpha \cdot \left(\mu_{mn}^2 + \left(\frac{\varepsilon_j}{h}\right)^2\right); \quad n, j = 1, 2, \ldots; m = 0, 1, 2, \ldots. \tag{9}$$

The response to Dirac's pulse induction in time domain $T_\delta(r, z, \theta, t)$ was obtained using the inverse Laplace's transformation and Bromwich integral, and it can be expressed in the following form:

$$T_\delta(r, z, \theta, t) = L^{-1}\{T^*(r, z, \theta, s)\} = \int_{p-i\infty}^{p+\infty} T^*(r, z, \theta, s) \cdot \exp(st) \cdot ds \Rightarrow$$

$$T_\delta(r, z, \theta, t) = \frac{2 \cdot \alpha \cdot A}{h\lambda} \sum_{m,n,j=1}^{N} J_m(\mu_{mn}r) E_j(z) \cdot (c_{1mn} \cos(m\theta) + c_{2mn} \sin(m\theta)) \exp\left(\frac{-t}{\tau_{mnj}}\right), \tag{10}$$

where p is the positive real parameter; L^{-1} denotes the inverse Laplace's transformation; τ_{mnj} and $E_j(z)$ are given by the next relations:

$$\tau_{mnj} = \frac{1}{\alpha \left(\mu_{mn}^2 + \left(\frac{\varepsilon_j}{h} \right)^2 \right)}; \quad E_j(z) = \frac{\lambda \varepsilon_j \cos \varepsilon_j (1 - z/h) + h_c \cdot h \sin \varepsilon_j (1 - z/h)}{(\lambda + h_c \cdot h) \sin \varepsilon_j + \lambda \varepsilon_j \cos \varepsilon_j}. \tag{11}$$

The Bromwich integral was evaluated using the contour integration; the contour of the integration, in the complex plane, is shown in Fig. 2.

Also, for a cylinder with infinite length the next relation holds:

$$T_\delta = \frac{A}{\lambda} \sqrt{\frac{\alpha}{\pi \cdot t}} \cdot \exp \left(\frac{-z^2}{4\alpha \cdot t} \right) \sum_{m,n=1}^{N} J_m(\mu_{mn} r) \cdot (c_{1mn} \cos(m\theta) + c_{2mn} \sin(m\theta)) \exp(-\mu_{mn}^2 \cdot \alpha \cdot t). \tag{12}$$

For arbitrary time dependence of the laser beam intensity, the temperature distribution inside the specimen could be evaluated by a convolution integral as [9,12]:

$$T(r, z, \theta, t) = \int_0^t \phi(t - \tau) \cdot T_\delta(r, z, \theta, \tau) \cdot d\tau. \tag{13}$$

If the laser beam has rounded cross-section, top head profile and constant intensity I_0 in time, because of symmetry, (Fig. 3) the temperature distribution would be an odd function of angular coordinate and in that way the temperature difference could be expressed in the following way:

$$T(r, z, \theta, t) = \frac{2\alpha \cdot A \cdot I_0}{h\lambda} \sum_{m,n,j=1}^{N} c_{1mn} J_m(\mu_{mn} r) \tau_{mnj} E_j(z) \cos(m \cdot (\theta - \theta_0)) \left(1 - \exp \left(\frac{-t}{\tau_{mnj}} \right) \right), \tag{14}$$

where θ_0 and r_1 are angular and radial coordinates respectively, of the center of the laser beam.

The τ_{mnj} and $E_j(z)$ in expression (14) have the same meaning as in (10).

The above results could be used in heating as well as cooling processes provoked by the laser beam [8].

As could be seen from relation (9) all poles are real and negative, thus all temporal terms in relations (10) and (14) will be convergent. The rate of the convergence, of these terms, is dependent on the value of the quotient t/τ_{mnj}, where t is the duration of the laser pulse, and τ_{mnj} is given in (11).

To estimate the number of terms in series (14), needed for preset accuracy for the temperature value, the relative difference δ between two temperatures at the same point and the same time for two different numbers of the terms in the sum, could be defined by the next relation:

$$\delta_N = \frac{|T_N - T_{N+M}|}{T_{N+M}}, \tag{15}$$

where T_N and T_{N+M} are the temperature values at the same position for two different sum boundaries in the relation (14), N and $N + M$, respectively.

In Fig. 4. the relative difference δ as a function of the number N in (14) for three different time durations Δt of the laser pulse, for $M = 25$, and for an Al specimen is shown.

The considered point is in the center of the beam and the laser beam with top head profile was assumed to have the following characteristics: power = 500 W; radius = 1 mm, coordinate of the laser beam center: $\theta_0 = 0$; $r_1 = 4$ mm, and the dimensions of the Al specimen are $h = 5$ mm; $R = 7$ mm.

As could be seen from the above figures, for a very short laser pulse, the sum in relation (14) converges slowly, and a very large number of the terms in the series has to be taken into account. As the above considerations are valid only for heating of the material, before melting or other disintegration processes started, for high intensity of the laser beam, short laser pulses have to be considered, and in this case the presented numerical procedure becomes computationally expensive.
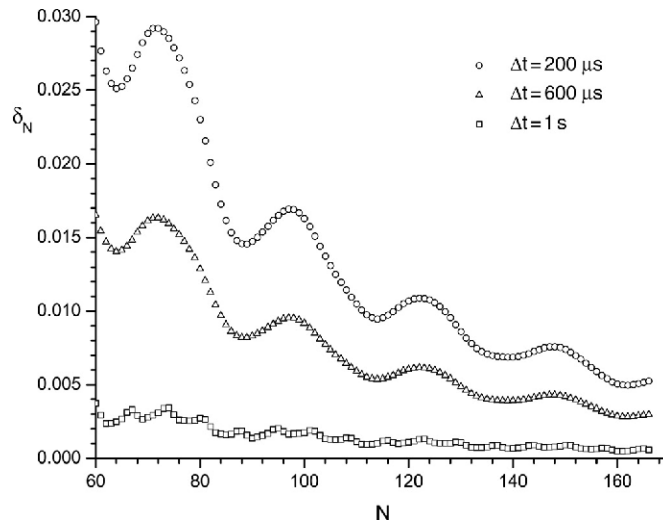
Fig. 4. The relative difference δ given in (15) at the center of the laser beam as a function of number N in relation (14), for $M = 25$ and for three different time durations Δt of the laser beam. The laser beam properties: power = 500 W, radius = 1 mm, position $\theta_0 = 0$; $r_1 = 4$ mm.

3. Numerical examples

In this section according to the above considerations numerical examples are presented for some characteristic cases. A cylindrical Al specimen is considered and the following characteristic parameters were assumed:

$\lambda = 240$ [W/K m]; $\quad \rho = 2700$ [kg/m^3]; $\quad c = 1021.71$ [J/kg K]; $\quad h_c = 10$ [W/K m^2]; $\quad A = 0.64$;

$h = 5$ [mm]; $\quad R = 7$ [mm].

In all numerical examples the number of terms (N) in the series in relation (14), for preset margin, could be estimated using the relative difference δ from Fig. 4, which in this case was estimated to be $N = 80$.

In Figs. 5 and 6 the contour lines and distributions for the temperature field on the upper surface (X–Y plane) of the specimen are presented, respectively. The laser beam with top head profile was assumed to have the following characteristics: power = 500 W; radius = 1 mm; time duration = 1 s, coordinates of the laser beam center: $\theta_0 = 0$; $r_1 = 4$ mm.

In Figs. 7 and 8 the contour plot and the distribution of the temperature field in X–Z plane are presented, respectively. The laser beam and the specimen parameters are the same as in the case shown in Figs. 5 and 6.

In Figs. 9 and 10 the contour plot and the distribution of the temperature difference on the upper surface (X–Y plane) were presented, respectively, for the case of two laser beams with the same top head profiles. The laser beams have the following properties: powers $P_1 = 500$ W, $P_2 = 500$ W; radii: $r_{01} = r_{02} = 0.5$ mm; time duration 1 s, positions of the laser beam's center: $r_1 = 2$ mm, $\theta_{01} = 0$ rad; $r_2 = 3.2$ mm, $\theta_{02} = 0$ rad.

In Fig. 11 the contour plot in the X–Z plane, for the same case, was presented. The dimensions and assumed physical properties of the specimen were the same as in the previous cases.

The results show that the presented approach is suitable for modeling of material heating by two or more beams in different positions or the multi-mode working regime.

In Fig. 12 the contour plot on the upper side (X–Y plane) of the specimen was shown for a case of two different laser beams. The laser beam properties for this case are: powers $P_1 = 500$ W, $P_2 = 350$ W; radii: $r_{01} = 1$ mm and $r_{02} = 0.7$ mm; time duration 1 s, positions of the laser beam centers: $r_1 = 4$ mm, $\theta_{01} = 0$ rad; $r_2 = 3.5$ mm, $\theta_{02} = \frac{\pi}{4}$ rad. The dimensions and assumed physical properties of the specimens were the same as in the previous cases.

4. Conclusions

An analytical approach for solving 3D problems of heating of material with a laser beam was considered. The heating process was modeled using the linear non-stationary heat equation applied to cylindrical geometry. The spatial
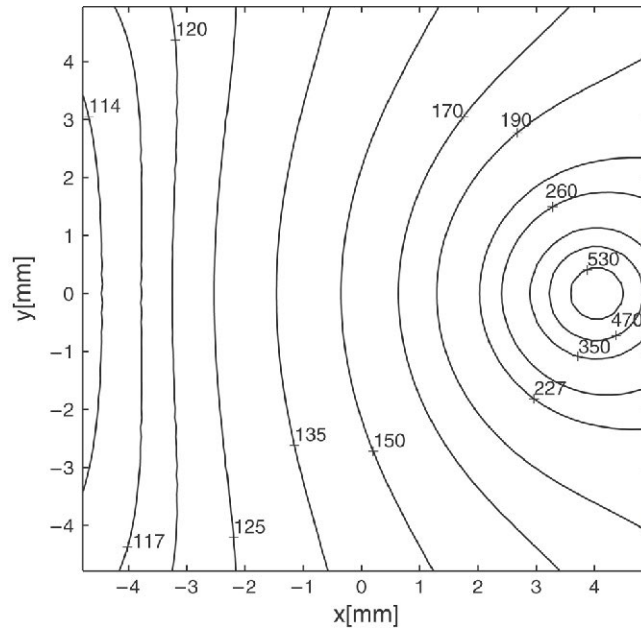
Fig. 5. The contour plot on the upper surface of the specimen for the laser beam properties: power $= 500$ W, radius $= 1$ mm, time duration $= 1$ s, position $\theta_0 = 0$; $r_1 = 4$ mm.
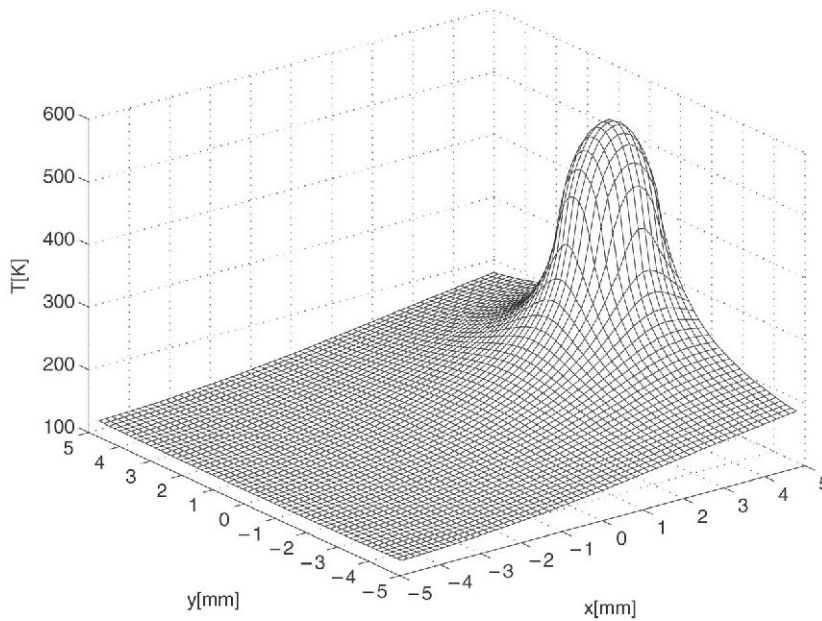

Fig. 6. Temperature field distribution on the upper surface of the specimen for the laser beam properties: power $= 500$ W, radius $= 1$ mm, time duration $= 1$ s, position $\theta_0 = 0$; $r_1 = 4$ mm.

and temporal distributions of the temperature fields were considered. Using the method of variable separations and the Laplace transformation, the governing PDE with corresponding BC and IC was solved and the temperature field distributions were presented in closed form.

By using an appropriate set of orthogonal functions, the numerical procedure was made more effective, producing a saving in CPU time. The obtained numerical results improved as the number of terms used in the series of the solution increased.
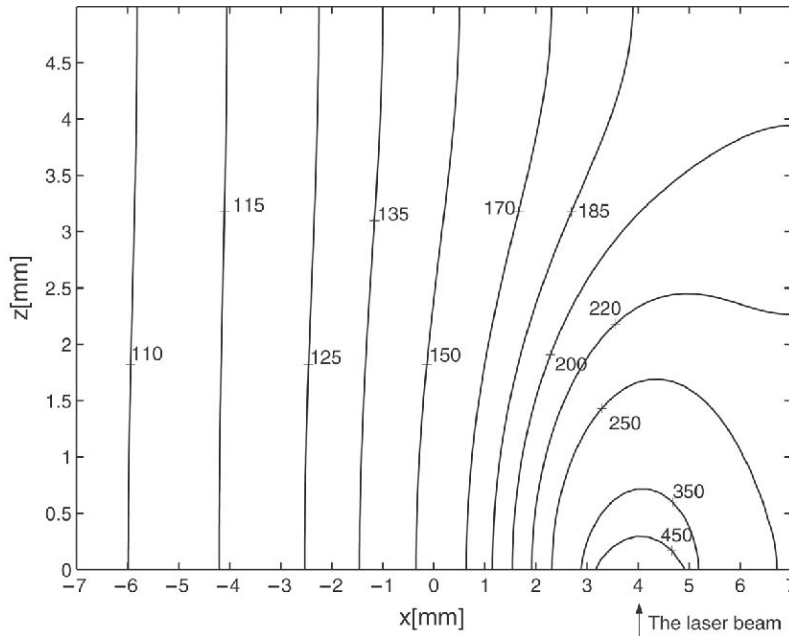
Fig. 7. Contour plot in the X–Z plane for the laser beam properties: power $= 500$ W, radius $= 1$ mm, time duration $= 1$ s, position $\theta_0 = 0$; $r_1 = 4$ mm.
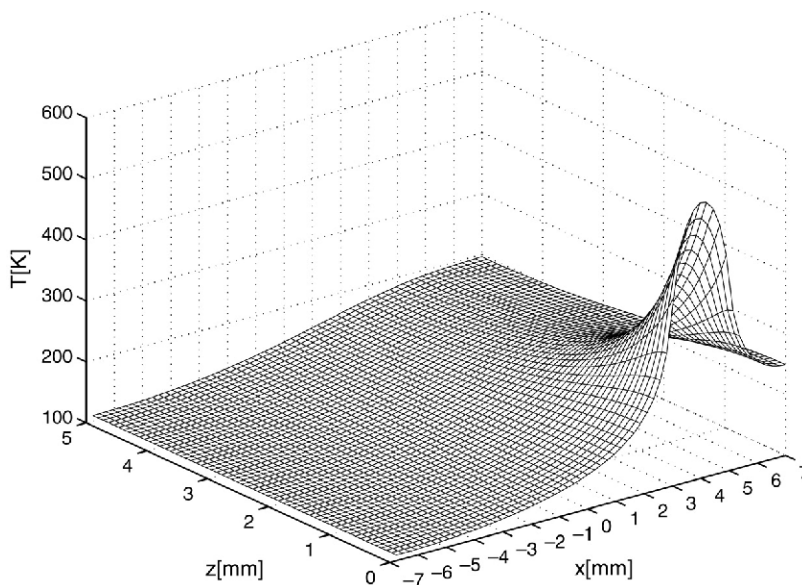

Fig. 8. Distribution of the temperature field in the X–Z plane for the laser beam properties: power $= 500$ W, radius $= 1$ mm, time duration $= 1$ s, position $\theta_0 = 0$; $r_1 = 4$ mm.

The convergence of the solutions was analyzed. For a short laser pulse the presented solutions converge slowly, and became computationally expensive.

Numerical examples were presented for the Al specimen with different characteristic positions of the laser beam. The convolution integral and Duhamel's principle can be used to represent arbitrary time dependence of the laser beam intensity.

For complex profiles of the laser beam the superposition principle was used. The temperature field distribution was considered and presented for two different laser beams targeting the same specimen.
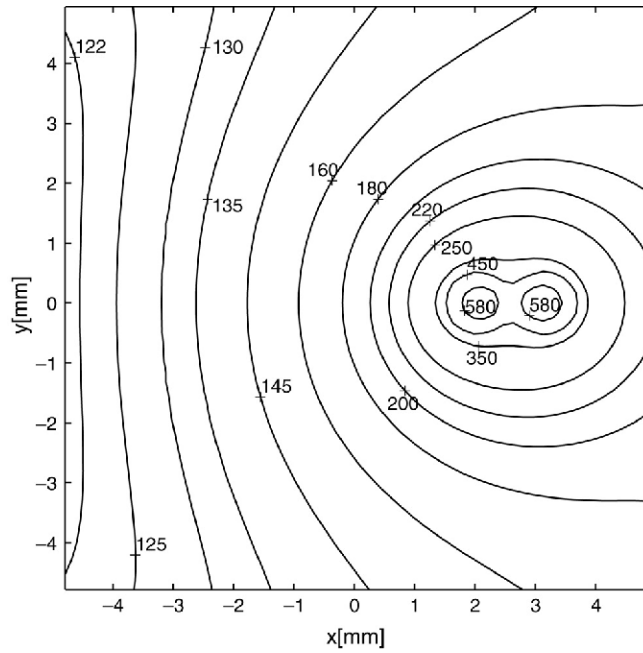
Fig. 9. Contour plot on the upper surface of the specimen, for two incident laser beams, with positions of the laser beams: $r_1 = 2$ mm, $\theta_{01} = 0$ rad; $r_2 = 3.2$ mm, $\theta_{02} = 0$ rad.
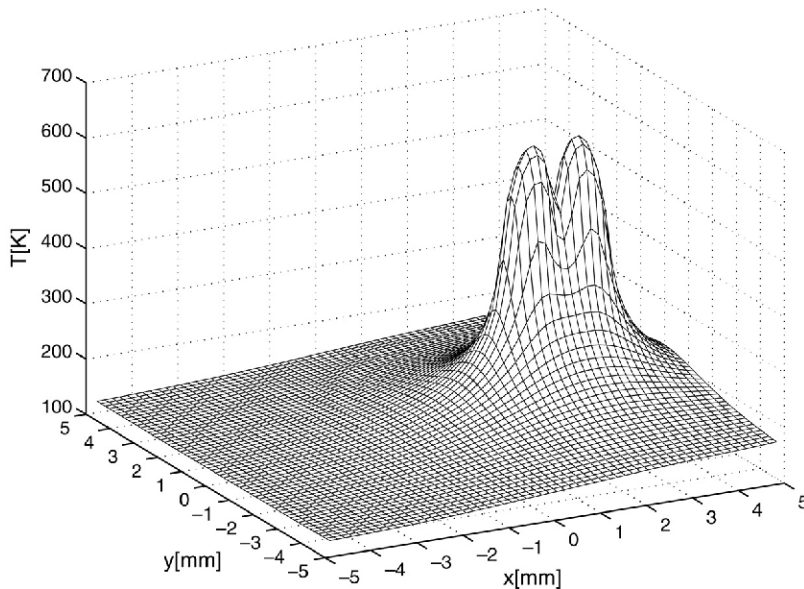

Fig. 10. Distribution of the temperature field on the upper surface of the specimen for two incident laser beams, with positions of the laser beams: $r_1 = 2$ mm, $\theta_{01} = 0$ rad; $r_2 = 3.2$ mm, $\theta_{02} = 0$ rad.

The presented approach could be of interest in many practical applications, especially in cases such as multi-mode working regimes of lasers and asymmetrical distribution of the laser beam intensity. Also, developed solutions could be used in the case of the moving laser beam. In this case the coordinates of the center of the laser beam, as a function of time, could be approximated by the step-functions. In this way, using the superposition principle, for each different position of the laser beam, temperature distributions could be evaluated.
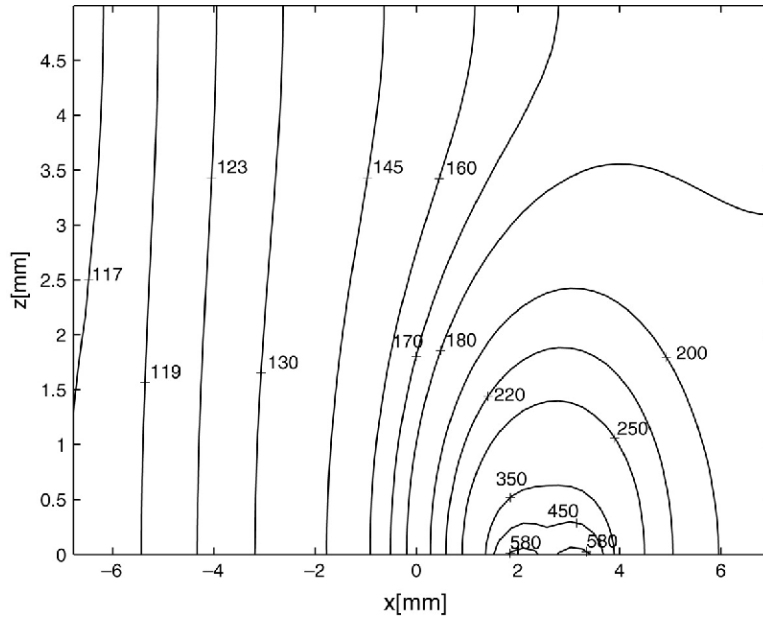
Fig. 11. Contour plot in the $X-Z$ plane, for two incident laser beams, with position of the laser beams: $r_1 = 2$ mm, $\theta_{01} = 0$ rad; $r_2 = 3.2$ mm, $\theta_{02} = 0$ rad.
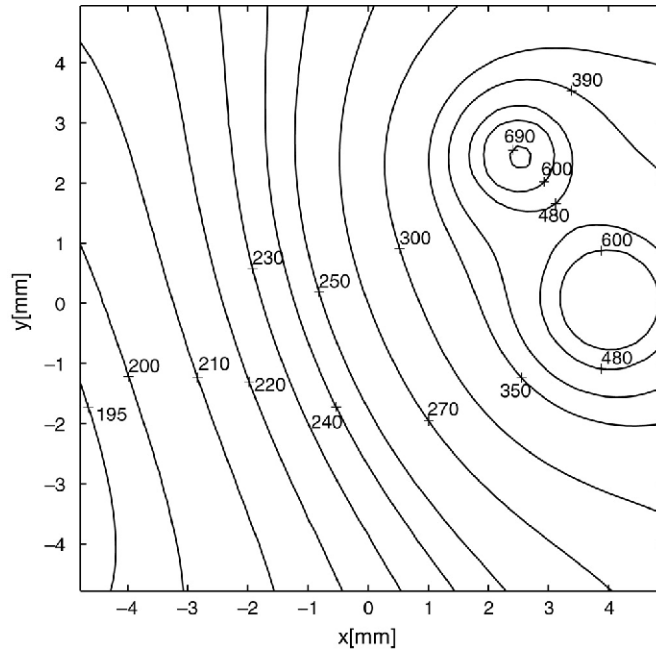

Fig. 12. Contour plot for the temperature distribution on the upper surface of the specimen ($X-Y$ plane), with positions of the laser beams: $r_1 = 4$ mm, $\theta_{01} = 0$ rad; $r_2 = 3.5$ mm, $\theta_{02} = \frac{\pi}{4}$ rad.

The presented analytical solutions offer further advantages relative to direct monitoring since measurement of the temperature field distribution inside the bulk of the material is difficult to arrange and can be usually performed in a restricted number of points.

References

[1] T. Thorslund, F.J. Kahlen, A. Kar, Temperatures, pressures and stress during laser shock processing, Optics and Lasers in Engineering 39 (2003) 51–71.

[2] S.J. Farlow, Partial Differential Equations for Scientists and Engineers, Dover Publications, Inc., New York, 1993.

[3] R.M. Wood, Laser Damage in Optical Materials, Adam Hilger, Bristol, Boston, 1986.

[4] E.M. Bass, Laser Material Processing, North Holland, Amsterdam, 1983.

[5] S. Bojanic, Analyzing of laser–material interaction with condensed matter at viewpoint of physical models, Ph.D. Thesis, The Faculty of Electrical Engineering, University of Belgrade, Belgrade, 1997.

[6] C.A. Brebbia, J.C.F. Telles, L.C. Wrobel, Boundary Element Techniques, Springer-Verlag, Berlin, 1984.

[7] L.R. Ram-Moham, Finite Element and Boundary Element Applications in Quantum Mechanics, Oxford University Press, New York, 2002.

[8] N. Rykalin, A. Uglov, A. Kokora, Laser Machining and Welding, MIR Publishers, Moscow, 1978.

[9] R. Gospavic, M. Sreckovic, V. Popov, Modeling of laser–material interaction using semi-analytical approach, Mathematics and Computers in Simulations 65 (2004) 211–219.

[10] R.A. Flinn, P.K. Trojan, Engineering Materials and their Application, Houghton Mifflin Company, Boston, 1975.

[11] Y. Toyozawa, Optical Processes in Solids, Cambridge University Press, New York, 2003.

[12] E. Kreyzig, Advanced Engineering Mathematics, John Wiley & Sons, New York, 1983.

[13] E. Jahnke, F. Emde, F. Lösch, Special Functions, Nauka, Moscow, 1968.

[14] M. Abramovic, I.A. Stegun, Handbook of Mathematical Functions, Dover publications, Inc., New York, 1972.